Acta Pharmacologica Sinica

ARTICLE

Chemokine CCL2 promotes cardiac regeneration and repair in myocardial infarction mice via activation of the JNK/STAT3 axis

Wei Wang[1,2], Xiao-kang Chen[1,2], Lu Zhou[1,2], Feng Wang[1,2], Yan-ji He[1,2], Bing-jun Lu[1,2], Ze-gang Hu[3], Zhu-xin Li[1,2], Xue-wei Xia[1,2], Wei Eric Wang[4], Chun-yu Zeng[1,2,5,6]✉ and Liang-peng Li[1,2]✉

Stimulation of adult cardiomyocyte proliferation is a promising strategy for treating myocardial infarction (MI). Earlier studies have shown increased CCL2 levels in plasma and cardiac tissue both in MI patients and mouse models. In present study we investigated the role of CCL2 in cardiac regeneration and the underlying mechanisms. MI was induced in adult mice by permanent ligation of the left anterior descending artery, we showed that the serum and cardiac CCL2 levels were significantly increased in MI mice. Intramyocardial injection of recombinant CCL2 (rCCL2, 1 μg) immediately after the surgery significantly promoted cardiomyocyte proliferation, improved survival rate and cardiac function, and diminished scar sizes in post-MI mice. Alongside these beneficial effects, we observed an increased angiogenesis and decreased cardiomyocyte apoptosis in post-MI mice. Conversely, treatment with a selective CCL2 synthesis inhibitor Bindarit (30 μM) suppressed both CCL2 expression and cardiomyocyte proliferation in P1 neonatal rat ventricle myocytes (NRVMs). We demonstrated in NRVMs that the CCL2 stimulated cardiomyocyte proliferation through STAT3 signaling: treatment with rCCL2 (100 ng/mL) significantly increased the phosphorylation levels of STAT3, whereas a STAT3 phosphorylation inhibitor Stattic (30 μM) suppressed rCCL2-induced cardiomyocyte proliferation. In conclusion, this study suggests that CCL2 promotes cardiac regeneration via activation of STAT3 signaling, underscoring its potential as a therapeutic agent for managing MI and associated heart failure.

Keywords: myocardial infarction; CCL2; cardiomyocyte proliferation; Bindarit; STAT3; PF-4136309; stattic; neonatal rat ventricle myocytes

Acta Pharmacologica Sinica (2024) 45:728–737; https://doi.org/10.1038/s41401-023-01198-0

INTRODUCTION

Myocardial infarction (MI) and subsequent heart failure are leading causes of death worldwide [1]. Certain species, such as zebrafish, and neonatal mammals are capable of cardiac regeneration following myocardial injury through the proliferation of pre-existing cardiomyocytes [2, 3]; however, regeneration of adult mammalian heart tissue after injury is difficult to achieve, leading to an increased likelihood of heart failure [4–6]. Therefore, stimulating adult cardiomyocyte proliferation is a promising therapeutic strategy for treating MI.

Recent studies have highlighted inflammatory cells and cytokines as key drivers of cardiac regeneration [7]. In the context of cardiac inflammation following MI, C-C motif chemokine ligand 2 (CCL2), also known as monocyte chemoattractant protein 1 (MCP1), is one of the most significantly upregulated cytokines [8]. CCL2 levels in plasma and heart tissue are elevated in animals and humans with MI [9–11], and cardiac over-expression of CCL2 attenuates cardiac dysfunction and enhances cardiac healing [12]. However, it is not known whether CCL2 regulates cardiomyocyte proliferation.

Here, we show that elevation of CCL2 levels in mouse plasma and heart post-MI positively regulates cardiac regeneration, and that the underlying mechanisms by which CCL2 contributes to cardiomyocyte proliferation are mediated by JNK/STAT3 signaling.

MATERIALS AND METHODS

Animal experiments

Animal care and treatment were performed in strict accordance with the approved protocols and animal welfare regulations of the Laboratory Animal Welfare and Ethics Committee of the Army Medical University (Approved Number. AMUWEC20219009). An

[1]Department of Cardiology, Daping Hospital, The Third Military Medical University (Army Medical University), Chongqing 400042, China; [2]Key Laboratory of Geriatric Cardiovascular and Cerebrovascular Disease Research, Ministry of Education of China; Chongqing Key Laboratory for Hypertension Research, Chongqing Cardiovascular Clinical Research Center, Chongqing Institute of Cardiology, Chongqing 400042, China; [3]Department of Laboratory Animal Center, Daping Hospital, The Third Military Medical University (Army Medical University), Chongqing 400042, China; [4]Department of Geriatrics, Southwest Hospital, The Third Military Medical University (Army Medical University), Chongqing 400038, China; [5]State Key Laboratory of Trauma, Burns and Combined Injury, Daping Hospital, The Third Military Medical University (Army Medical University), Chongqing 400042, China and [6]Cardiovascular Research Center of Chongqing College, Chinese Academy of Sciences, University of Chinese Academy of Sciences, Chongqing 400714, China
Correspondence: Chunyu Zeng (chunyuzeng01@163.com) or Liangpeng Li (liangpengli@163.com)
These authors contributed equally: Wei Wang, Xiao-kang Chen

Received: 20 June 2023 Accepted: 12 November 2023
Published online: 12 December 2023

adult mouse MI model was induced in 8-week-old C57BL/6 J mice as described previously. Briefly, hair was removed from the surgical area of the neck and chest 1 day before surgery. Mice were anesthetized by 5% isoflurane inhalation in an airtight chamber and were then disinfected with a povidone iodine solution. Tracheal intubation was performed, and mice were artificially ventilated using a volume-controlled ventilator with 2.4% isoflurane/97.6% oxygen. A thoracotomy was performed to expose the heart and the proximal left anterior descending coronary artery. Mice were subjected to permanent ligation of the left anterior descending artery using a 7-0 polypropylene suture. The sham group underwent the same surgical procedure except that the proximal left anterior descending coronary artery was not occluded. Mice were administered an intramyocardial injection of recombinant CCL2 protein (20 μL at 50 μg/mL, Cat. #279-MC/CF, R&D systems, Rochester, Minnesota, USA) or PBS at the border region of the infarct with a 30-gauge needle immediately after surgery.

Echocardiography

Heart function was evaluated by echocardiography at 1, 7, 14, 21, and 28 days after proximal left anterior descending coronary artery ligation. Mice were placed on a heated platform in the supine position and then sedated by isoflurane inhalation (100 mg/kg). 2D clips and M-mode images were recorded by using a Vevo 3100 LT device (Fujifilm VisualSonics, Bothell, WA, USA). Ejection fraction (EF %) and fractional shortening (FS %) were calculated from left ventricle dimensions in the 2D long-axis view. All echocardiography measurements were performed in a blinded manner.

Isolation of primary cardiomyocytes

Primary cardiomyocytes were isolated from 1-day-old (P1) and 7-day-old (P7) Sprague-Dawley rats as previously described. Briefly, ventricles from P1 and P7 neonatal rats were minced into small pieces and digested in PBS buffer or ADS buffer [0.68% NaCl (*w/v*), 0.476% HEPES (*w/v*), 0.012% NaH_2PO_4 (*w/v*), 0.1% glucose (*w/v*), 0.04% KCl (*w/v*), 0.01% $MgSO_4$ (*w/v*), pH 7.35] containing 0.8 mg/mL collagenase II (Worthington Biochemical Corporation, Lakewood, NJ, USA) and 1.25 mg/mL trypsin (Sigma-Aldrich, Darmstadt, Germany) with shaking at 37 °C. Samples were then centrifuged for 5 min at 300 × *g* and cells were re-suspended in complete medium (Dulbecco's modified Eagle's medium with 4.5 g/L *D*-Glucose, Gibco, New York, NY, USA). Cardiomyocytes were enriched (>90% purity) by a 2-h pre-plating step in 100-mm dishes in complete medium at 37 °C with 5% CO_2 to remove cardiac fibroblasts. Unattached cardiomyocytes were collected and plated on laminin-coated Millicell EZ slides (Millipore, Burlington, MA, USA) and incubated for 24 h at 37 °C with 5% CO_2 to allow cell attachment. Cells were then exposed to the following treatments: recombinant CCL2 (100 ng/mL, Cat. #279-MC/CF, R&D systems), Bindarit (CCL2 inhibitor, 30 μM, Cat. #B129927, Aladdin, Riverside, CA, USA), PF-4136309 (CCR2 antagonist, 30 μM, Cat. #HY-13245, MCE, Monmouth Junction, NJ, USA), Stattic (STAT3 inhibitor, 30 μM, #HY-13818, MCE).

Histology and immunofluorescence staining

C57BL/6 J mice were euthanized at specified times and hearts were harvested and fixed in 4% paraformaldehyde for 24 h at room temperature, infiltrated and embedded in paraffin blocks. For histology and immunofluorescence staining, embedded hearts were sectioned at a thickness of 4 μm. Masson's trichrome staining was performed according to a standard protocol. Scar size was quantified by ImageJ software, based on Masson's trichrome staining. Immunofluorescence staining was performed on both paraffin sections and plated primary cardiac cells. Sections or cardiomyocytes were incubated overnight at 4 °C with primary antibodies: anti-cardiac troponin T (Cat. # MA5-12960, mouse, Invitrogen, Carlsbad, CA, USA), anti-Ki67 (Cat. #9129 S, rabbit, Cell Signaling Technology, Danvers, MA, USA), anti-phosphor histone H3 (Ser10) conjugated with Alexa Fluor 555 (Cat. #3475 S, rabbit, Cell Signaling Technology,), anti-Aurora B (Cat. #ab2254, rabbit, Abcam, Cambridge, UK), anti-CCL2/MCP1 (Cat. #ab25124, rabbit, Abcam), anti-CCR2 (Cat. #ab203128, rabbit, Abcam), and anti-CD31 (Cat. #ab281583, rabbit, Abcam). Sections were rinsed and incubated with corresponding secondary antibodies conjugated to Alexa Fluor 488 (Cat. #A-21202, Invitrogen) or Alexa Fluor 555 (Cat. #A10040, Invitrogen) for 1 h at 37 °C. In the final 10 min of this incubation, 4′,6-diamidino-2-phenylindole (DAPI) dye solution (Solarbio, Beijing, China) was added for nuclear staining. To calculate the rate of cardiomyocyte proliferation in vitro, we counted the total number of cardiomyocytes and the number of Ki67-, PH3- and Aurora B-positive cardiomyocytes in different positions and at least 10 fields for each group. In all cell counting experiments, fields of view were randomized to reduce counting bias. The mean fluorescence intensity was calculated by ImageJ software.

TUNEL assay

The terminal deoxynucleotidyl transferase mediated dUTP-biotin nick end labeling (TUNEL) assay was conducted using an In Situ Cell Death Detection Kit (Roche, Basel, Switzerland) according to the manufacturer's instructions. Heart sections were processed using the TUNEL kit at room temperature for 1 h in the dark to determine in vivo cardiomyocyte apoptosis after MI.

Enzyme-linked immunosorbent assay for CCL2 in plasma

Blood (50 μL) collected from the right heart ventricle of mice was added to 30 μL 250 mM EDTA and centrifuged at 4 °C for 15 min at 3000 × *g* to enable plasma collection. The level of CCL2 in plasma was determined using a mouse MCP1/CCL2 enzyme-linked immunosorbent assay (ELISA) kit (Cat. #CSB-E07430m, CUSABIO, Houston, TX, USA) following the manufacturer's instructions. Briefly, 100 μL samples were loaded onto the 96-well plates and incubated at 37 °C for 2 h. Then the plates were incubated with the primary antibody for another 2 h at 37 °C. After adding the substrate solution, the absorbance was measured by spectrophotometry using a microplate reader set to 450 nm.

Western blot analysis

Total protein was extracted using RIPA Lysis buffer (50 mM Tris pH 7.4, 150 mM NaCl, 1% Triton X-100, 1% sodium deoxycholate, 0.1% SDS, Beyotime). Protein concentration was determined using the Bicinchoninic Acid (BCA) Protein Assay Kit (Beyotime), with glyceraldehyde-3-phosphate dehydrogenase (GAPDH) serving as an internal control for total protein. Protein samples (50 μg) were then subjected to sodium dodecyl sulfate-polyacrylamide gel electrophoresis (SDS-PAGE) and subsequently transferred to nitrocellulose (NC) membranes (Bio-Rad Laboratories, Hercules, CA, USA). These membranes were blocked with 5% non-fat milk in Tris-buffered saline (10 mM Tris-HCl pH 7.5, 150 mM NaCl) containing 0.1% Tween 20 for 1 h at room temperature. This was followed by an overnight incubation at 4 °C with primary antibodies: anti-CCL2/MCP1 (Cat. #ab25124, rabbit, Abcam), anti-SAPK/JNK (Cat. #9252 T, rabbit, Cell Signaling Technology), anti-phosphor-SAPK/JNK (Cat. #4668 T, rabbit, Cell Signaling Technology), anti-STAT3 (Cat. #9139 S, mouse, Cell Signaling Technology), anti-phosphor-STAT3 (Cat. #9131 S, rabbit, Cell Signaling Technology), anti-cleaved-Caspase3 (p17/p19) (Cat. #19677-1-AP, rabbit, Proteintech, Wuhan, Hubei, China), and anti-GAPDH (Cat. #60004-1-Ig, mouse, Proteintech). After three washes in Tris-buffered saline, membranes were probed with secondary antibodies (IR Dye 800 CW, goat anti-rabbit, IR Dye 680 CW, goat anti-mouse, Li-Cor, Lincoln, NE, USA) for 1 h at room temperature. Protein bands were visualized using an Odyssey Imaging System.

Quantitative real-time PCR

Total RNA was extracted from cardiomyocytes using Trizol reagent. Reverse transcription (RT) was conducted using PrimeScript™ RT Master Mix (Takara Biomedical Technology, Beijing, China). Quantitative real-time PCR (qRT-PCR) was performed using SYBR® Premix Ex Taq™ II (Takara Biomedical Technology) and a Real-Time PCR system (Bio-Rad) following standard protocols. Expression levels of specific genes were normalized to that of *Gapdh*. The primers used were: for rat *Ccl2*: Forward (F): 5′-CATCAACCCTAAGGACTTCAGC-3′, Reverse (R): 5′-TCTACAGAAG TGCTT-GAGGTGG-3′; for mouse *Ccl2*: Forward (F): 5′-GCTGA CCCC-AAGAAGGAATG-3′, Reverse (R): 5′-GGTGGTTGTGGAAAGG-TAGTG-3′; for mouse *Gapdh*: Forward (F): 5′-CCACTCTTCCACCTTC-GATG-3′, Reverse (R): 5′-CCACCACCCTGTTGCTGTA-3′.

Endothelial tube formation assay

Pipette tips and 48-well plates were precooled, and growth-factor-reduced Matrigel (BD, Franklin Lakes, NJ, USA) was thawed overnight prior to the assay. The wells of the 48-cell plates were coated by incubation with 100 μL Matrigel for 30 min. Human umbilical vein endothelial cells (HUVECs) were starved in RPMI-1640 medium without serum for 24 h prior to the assay and then 2×10^4 HUVECs were seeded into each Matrigel-coated well. Tube formation by HUVECs was observed at different time points during a 12-h experimental period using light microscopy.

Statistical analysis

All data are presented as the mean ± SEM. Statistical analyses were conducted using GraphPad Prism 8.0 software, employing either one-way ANOVA or Student's *t*-test. A two-tailed *P* value of <0.05 was considered statistically significant.

RESULTS

CCL2 suppresses cardiac remodeling and promotes cardiac repair after MI

CCL2 levels in human plasma increase shortly after MI [11]; however, changes in CCL2 levels in mice following MI remain unclear. Our results showed that mouse plasma levels of CCL2 increased quickly, peaked at 3 days, and lasted until 14 days post-MI (Fig. 1a). To gain insight into the cardiac expression patterns of *Ccl2* following MI, we re-analyzed transcriptome data from C57BL/6 J mouse heart subjected to MI at different ages (GSE95755 and GSE123868) [13, 14]. The results showed that the fragments per kilobase of transcript per million mapped reads (FPKM) of cardiac *Ccl2* were significantly higher in injured myocardium compared with uninjured heart or heart areas remote from injury from P1, P8 and adult mice (Supplementary Fig. S1a–c). These data were confirmed by our real-time-PCR, immunoblotting, and immunofluorescence staining experiments (Fig. 1b, c, Supplementary Fig. S1d, e).

To investigate a potential role of elevated CCL2 in cardiac remodeling, we administered recombinant CCL2 (rCCL2) intramyocardially to C57BL/6 J mice subjected to MI at a dose of 50 μg/mL, with a total injection volume of 20 μL (Fig. 2a). Our results showed that rCCL2 significantly improved survival and cardiac function, and prevented ventricle remodeling 4 weeks post-MI, as assessed by echocardiography (Fig. 2b, c). Masson's trichrome staining also showed a remarkable decrease of scar size in mouse heart treated with rCCL2 (Fig. 2d). These findings indicate that elevated CCL2 levels may be protective against MI.

CCL2 inhibits cardiac apoptosis and promotes angiogenesis post-MI

Over-expression of CCL2 decreases glioma cell apoptosis by activating the AKT pathway [15]. We therefore investigated whether CCL2 influences cardiomyocyte apoptosis in injured myocardium. Using TUNEL staining and Western blot analysis of cleaved Caspase 3, we observed a reduction in cardiomyocyte apoptosis in the border zone of the myocardium infarct 7 days post-MI following rCCL2 administration (Fig. 3a, b).

While the role of CCL2 in endothelial cell function has been documented [16], its impact on angiogenesis following MI remains unreported. As revealed by CD31 immunofluorescence staining in heart sections 14 days post-MI, a mild increase in vascular density in the border zone was observed in the rCCL2-treated group compared with the vehicle-treated group (Fig. 3c). Endothelial tube formation assays further confirmed that rCCL2 promoted capillary-like tube formation in vitro (Fig. 3d). Endothelial cell proliferation is required for angiogenesis [17]; therefore, we also detected PH3 in endothelial cells, and found that rCCL2 boosted endothelial cell proliferation (Supplementary Fig. S2a, b). These data indicate that CCL2 may protect the heart from MI synergistically by the inhibition of cardiomyocyte apoptosis and the stimulation of angiogenesis.

CCL2 promotes cardiomyocyte proliferation

Inflammatory cytokines regulate cardiac regeneration; therefore, we investigated whether CCL2 alters cardiomyocyte proliferation. Our immunofluorescence staining results showed that CCL2 treatment increased the number of Ki67-, PH3- and Aurora B-positive cardiomyocytes both in injured myocardium (Fig. 4a–c), and in P1 and P7 neonatal rat ventricle myocytes (NRVMs) (Supplementary Figs. S3, S4a–c and Fig. 5a–c).

We also observed endogenous CCL2 expression in P1 NRVMs (Supplementary Fig. S5). Treatment with Bindarit, a selective inhibitor of CCL2 synthesis [18], suppressed both CCL2 expression and cardiomyocyte proliferation in P1 NRVMs (Supplementary Fig. S4d and Fig. 5d–f). These data indicate that promoting cardiomyocyte proliferation contributes to the beneficial effects of CCL2 on MI, and that elevated levels of cardiac CCL2 may be derived from cardiomyocytes themselves.

CCL2 induces cardiomyocyte proliferation by activating CCR2/JNK/STAT3 signaling

CCL2 activates downstream signaling pathways mainly through binding to its receptor, CCR2 [19, 20]. Therefore, we performed immunofluorescence staining and confirmed the presence of CCR2 in P1 NRVMs (Supplementary Fig. S5b). In the presence of the CCR2 antagonist, PF-4136309, rCCL2-induced cardiomyocyte proliferation was blocked (Fig. 6a, b).

c-Jun N-terminal kinase (JNK)/signal transducer and activator of transcription 3 (STAT3) signaling is activated downstream of CCR2 and is required for zebrafish heart regeneration [20, 21]. We therefore speculated that CCL2 may stimulate cardiomyocyte proliferation by activating JNK/STAT3 signaling. We found that rCCL2 increased the protein levels of phosphor-JNK (p-JNK) and phosphor-STAT3 (p-STAT3) (Fig. 6c). When treated with Sttatic, a STAT3 inhibitor [22], CCL2-induced cardiomyocyte proliferation in NRVMs was substantially blocked, as assessed by Ki67 and PH3 immunofluorescence staining (Fig. 6d, e). These results indicate that CCL2 promotes the proliferation of cardiomyocytes by activating CCR2/JNK/STAT3 signaling.

DISCUSSION

Cardiomyocyte loss is a foundation pathology of MI that eventually leads to heart failure [1, 4]. Though recent studies highlight the potential for existing cardiomyocytes to regenerate within the adult heart, this regenerative capacity is limited [23, 24]. Therefore, fostering cardiomyocyte proliferation post-MI is a major challenge. After MI, the heart experiences heightened inflammatory responses [25]. Of the cytokines involved, the C-C chemokine family, specifically CCL2, plays a pivotal role. CCL2 levels, which

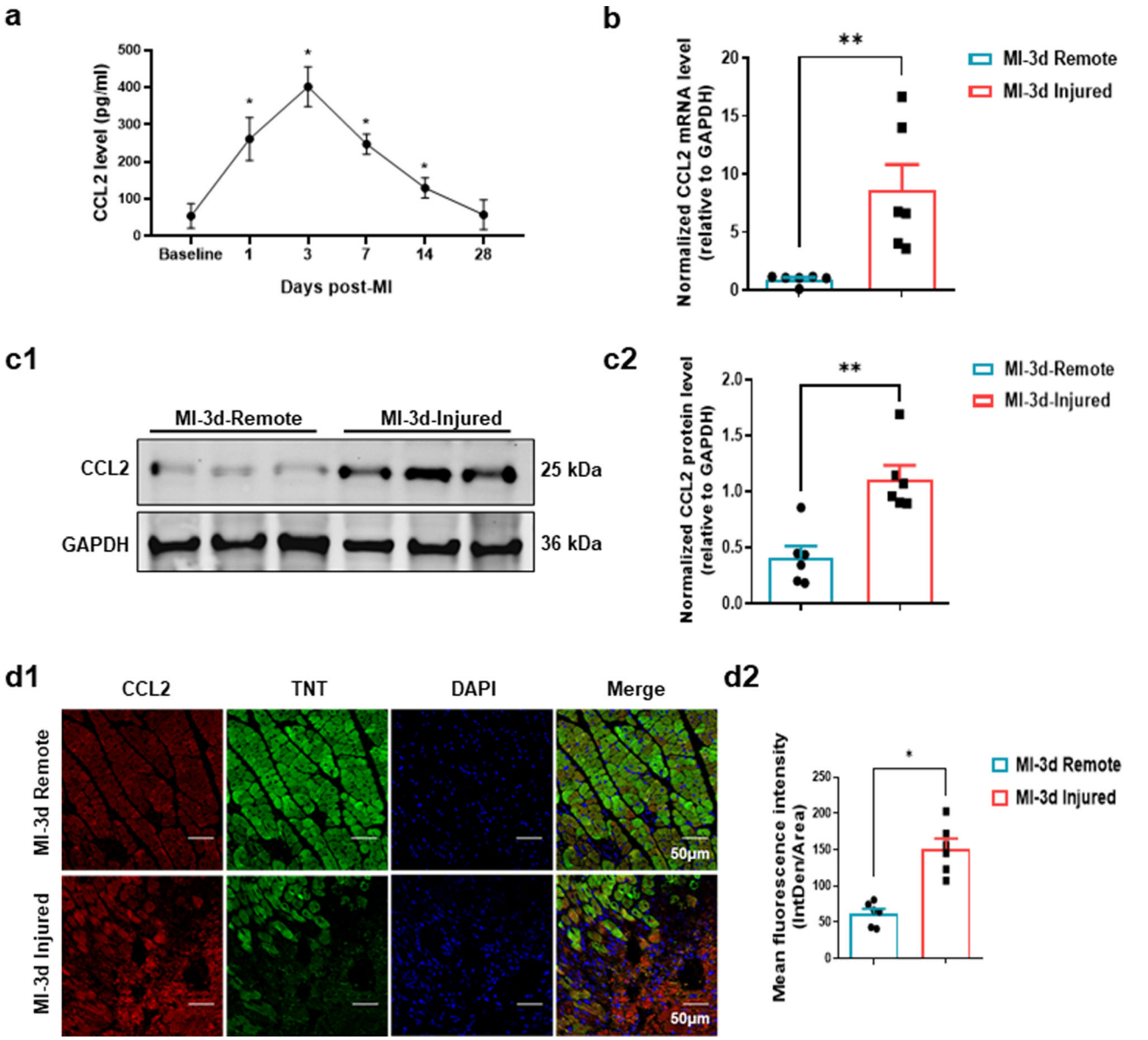

Fig. 1 CCL2 expression is increased in the mouse heart after MI. a ELISA measurement of plasma CCL2 after MI ($n = 6$, $^{*}P < 0.05$). Baseline indicates the level 1 day before MI. **b** *Ccl2* mRNA level in injured heart and in an area remote from injury at 3 days after MI ($n = 6$, $^{**}P < 0.01$). **c** Representative immunoblot image (**c1**) and quantification (**c2**) of CCL2 protein level in injured heart and in an area remote from injury at 3 days post-MI ($n = 6$, $^{**}P < 0.01$). **d** Representative immunofluorescence staining (**d1**) and mean fluorescence intensity (**d2**) of CCL2 in injured heart and in an area remote from injury at 3 days post-MI ($n = 6$, $^{**}P < 0.01$, scale bar = 50 μm). IntDen integrated density.

rise in the plasma following myocardial injury, have been identified to have prognostic value in both acute and chronic phases of acute coronary syndrome [26, 27], but its exact role in myocardial protection is not fully understood.

CCL2 can mitigate ventricular dysfunction post-injury and this beneficial effect might stem from its involvement in macrophage recruitment and activation, cytokine production, and myofibroblast accumulation in healing infarcts [12]. Conversely, the absence of MCP1 can lead to diminished post-infarction left-ventricular remodeling, but this occurs with a longer inflammatory phase and a delay in the replacement of damaged cardiomyocytes with granulation tissue [28]. Nevertheless, other studies have shown ischemia/reperfusion-induced CCL2 release causes cardiomyocyte apoptosis through monocyte chemotactic protein-induced protein 1 (MCPIP1) and calcium-sensing receptor pathways [29, 30]. This mirrors the nature of inflammation. While a well-orchestrated inflammatory response might be beneficial for myocardial repair, unchecked inflammation can have detrimental effects. Therefore, it is clear that a nuanced understanding of CCL2's multiple functions, as well as the contexts in which it operates, is vital. This will be instrumental in harnessing its potential benefits while mitigating potential risks in therapeutic applications.

Cardiac regeneration is largely regulated by inflammatory cells and cytokines secreted by inflammatory cells, such as oncostatin M [31]. However, the relationship between CCL2 and cardiac regeneration is unclear. Here, we showed that CCL2 levels are elevated both in mouse plasma and heart tissue post-MI. rCCL2 administration protected the heart from MI by inhibiting cardiomyocyte apoptosis, promoting angiogenesis, and importantly, stimulating cardiomyocyte proliferation. We further revealed that CCL2 and CCR2 are both expressed in primary

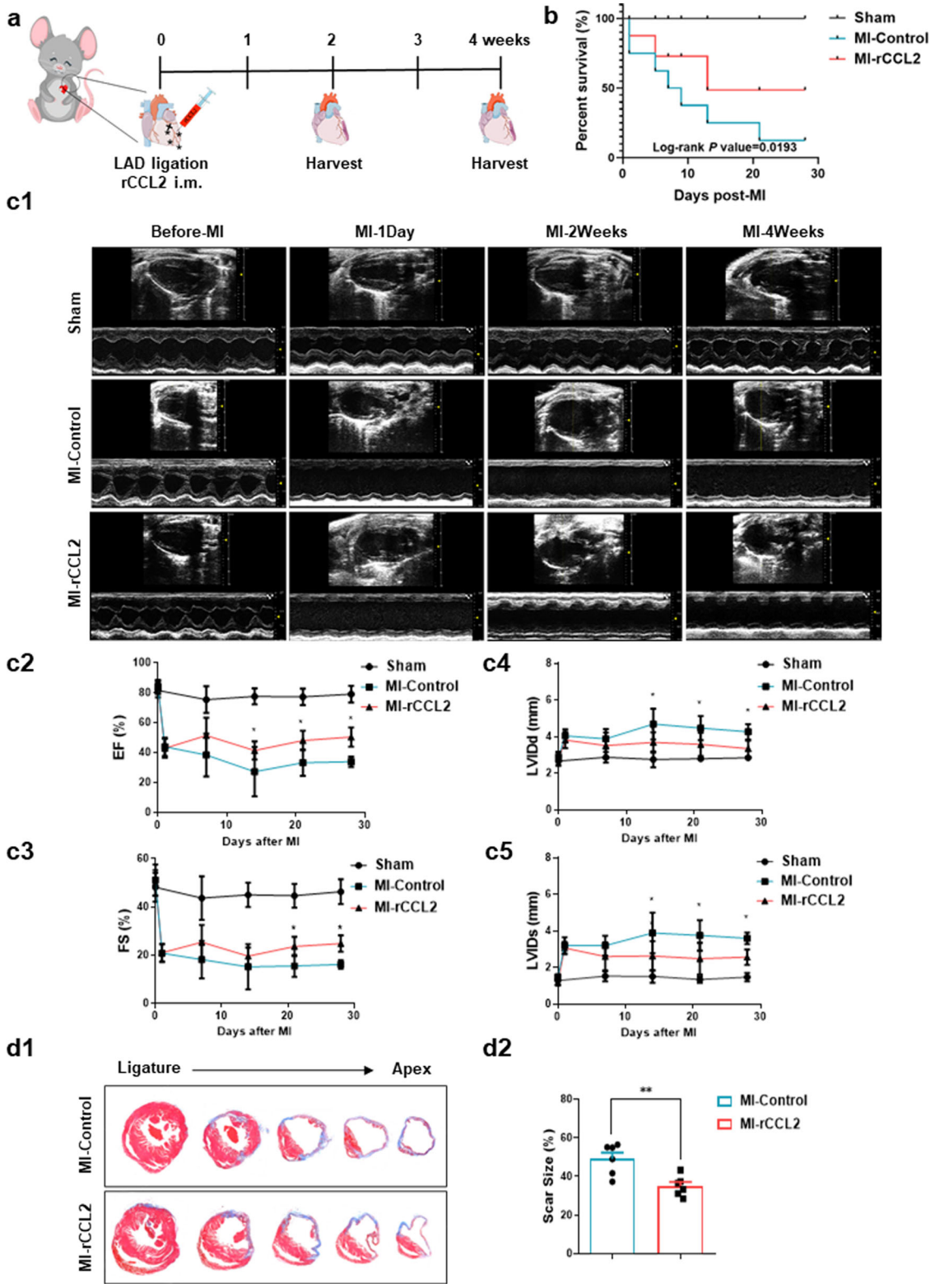

Fig. 2 CCL2 ameliorates cardiac remodeling after MI. a Schematic of intramyocardial injection of recombinant CCL2 and the experimental timeline to evaluate cardiac regeneration and cardiac function in the MI mouse model. **b** Recombinant CCL2 significantly improved the post-MI survival rate (Kaplan–Meier survival plot, $n = 6$). **c** Representative M-mode echocardiography (**c1**); ejection fraction (EF %), fractional shortening (FS %), left-ventricular end-diastolic internal diameter (LVIDd) and left-ventricular end-systolic internal diameter (LVIDs) (**c2**–**c5**) at 1, 7, 14, and 28 days post-MI ($n = 6$, $^{*}P < 0.05$). **d** Representative Masson's trichrome staining (**d1**) and quantification (**d2**) of scar area at 28 days after MI ($n = 6$, $^{**}P < 0.01$).

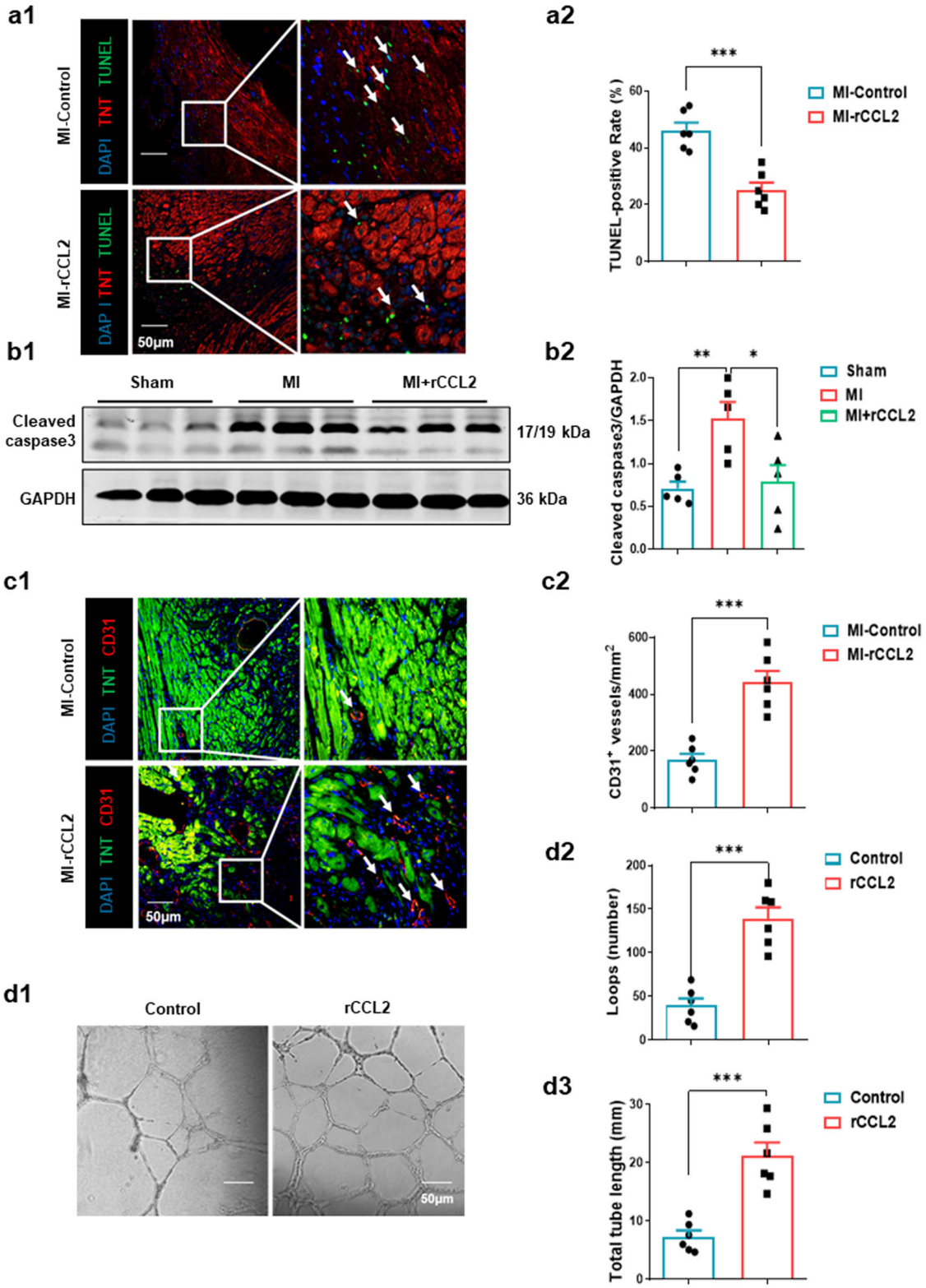

Fig. 3 **CCL2 promotes heart regeneration after MI. a** Representative images (**a1**) and quantification (**a2**) of TUNEL-positive cardiomyocytes in heart infarct border zone at 7 days post-MI ($n = 6$, $^{***}P < 0.001$, scale bar = 50 μm). **b** Representative immunoblot (**b1**) and quantification (**b2**) of cleaved-Caspase3 protein in heart at 3 days post-MI ($n = 6$, $^{**}P < 0.01$, $^{*}P < 0.05$). **c** Representative images (**c1**) and quantification (**c2**) showing CD31 immunofluorescence staining in heart sections at 14 days post-MI ($n = 6$, $^{***}P < 0.001$, scale bar = 50 μm). **d** Representative images (**d1**) and quantification (**d2**, **d3**) of endothelial tube formation assays ($n = 6$, $^{***}P < 0.001$, scale bar = 50 μm).

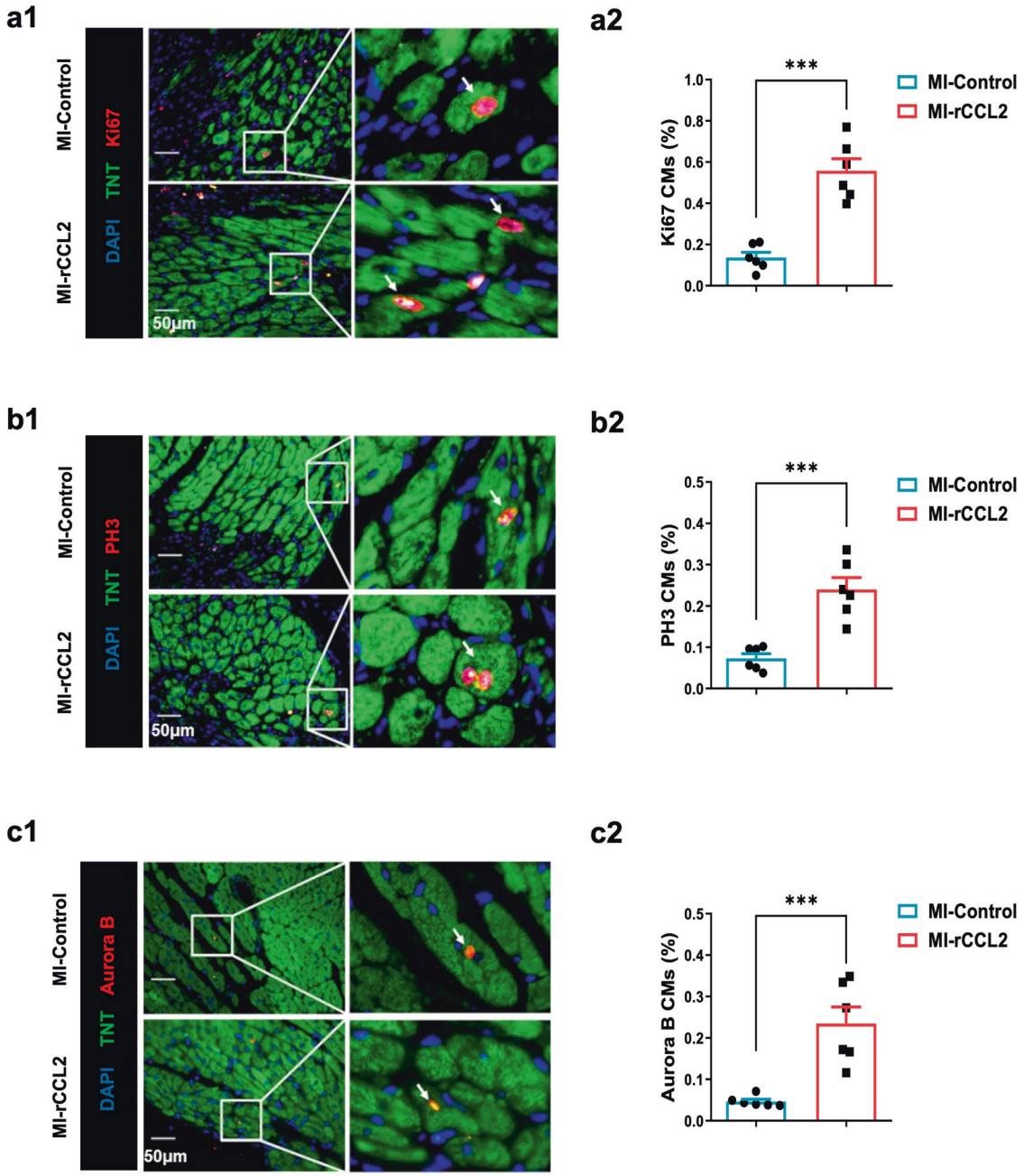

Fig. 4 CCL2 promotes cardiomyocyte proliferation in vivo. Representative immunofluorescence staining (**a1**, **b1**, **c1**) and quantification (**a2**, **b2**, **c2**) of Ki67, PH3, and Aurora B in the infarct area at 14 days post-MI ($n = 6$, $^{***}P < 0.001$, scale bar = 50 μm). CMs cardiomyocytes.

cardiomyocytes, and that the pharmacological inhibition of either CCL2 or CCR2 blunted cardiomyocyte proliferation in P1 NRVMs. This indicates that the increase in CCL2 plasma levels could be at least partially derived from cardiac tissue and is beneficial for cardiac regeneration.

In the signaling pathway downstream of CCL2, STAT3 plays a pivotal role in cardiac regeneration and is essential for the proliferation of cardiomyocytes [21, 32–35]. Our findings demonstrate that both JNK and STAT3 are activated in primary cardiomyocytes following rCCL2 administration. Furthermore, the proliferative response of cardiomyocytes to rCCL2 was significantly reduced upon STAT3 inhibition. Consequently, we deduce that the promotion of cardiomyocyte proliferation by CCL2 is, at least in part, because of activation of the JNK/STAT3 pathway.

Atherosclerosis is an inflammatory disease involving chemokines, among which CCL2 is prominent. Combined inhibition of CCL2, CX3CR1, and CCR5 abrogates Ly6C^{hi} and Ly6C^{lo} monocytosis and almost abolishes atherosclerosis in hypercholesterolemic mice [36]. Interestingly, loss of CCL2 in all Myh11^{+} smooth muscle cells results in a paradoxical increase in plaque size and macrophage content. CCL2, produced by smooth muscle cells and endothelial cells, decreases monocyte levels and acts in an athero-protective manner in the early stage of atherosclerosis. However, prolonged elevated production of CCL2 can intensify plaque pathogenesis in the advanced stages of the disease [37]. These inconsistent effects of CCL2 on atherosclerosis and cardiac regeneration mean that it is imperative to achieve precision and cardiac-specific targeting in CCL2 intervention techniques. Identifying the appropriate means to modulate CCL2 to optimize its protective benefits while

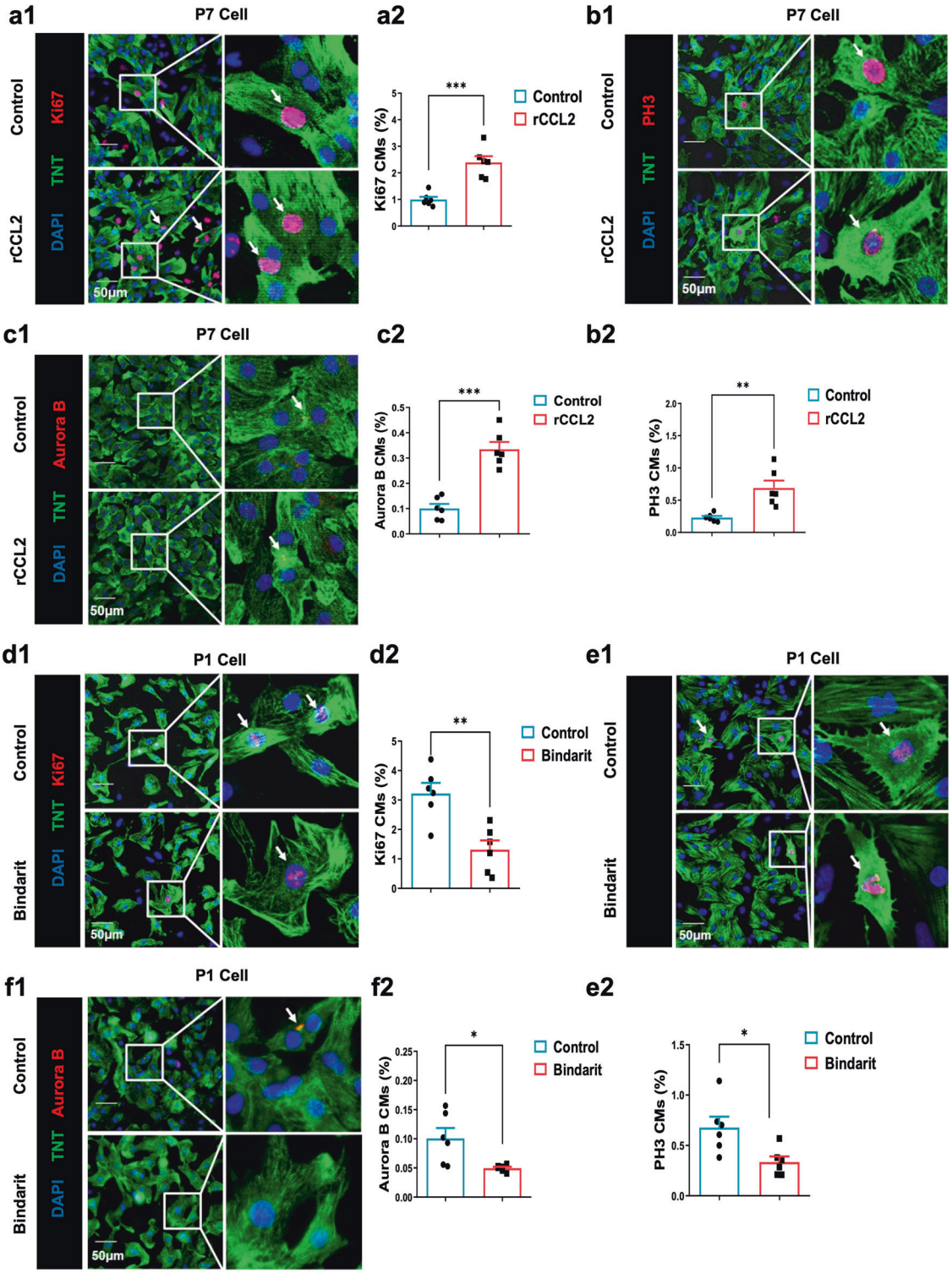

Fig. 5 CCL2 induces cardiomyocyte proliferation in vitro. a–c Representative images (**a1**, **b1**, **c1**) and quantification (**a2**, **b2**, **c2**) of Ki67, PH3 and Aurora B in P7 cardiomyocytes 24 h after recombinant CCL2 administration (100 ng/mL) ($n = 6$, $^{**}P < 0.01$, $^{***}P < 0.001$, scale bar = 50 μm). **d–f** Representative immunofluorescence images (**d1**, **e1**, **f1**) and quantification (**d2**, **e2**, **f2**) of Ki67, PH3 and Aurora B in P1 cardiomyocytes after treatment with Bindarit (30 μM) ($n = 6$, scale bar = 50 μm, $^{**}P < 0.01$, $^{*}P < 0.05$, scale bar = 50 μm). CMs cardiomyocytes.

minimizing its adverse effects should be a central concern of future research.

A limitation of this study is the absence of human-related experimental data. We also realize that the concentration changes of plasma CCL2 levels could not indicate its clinic significance, therefore, a series of randomized controlled clinic trials is needed to investigate the relationship between plasma CCL2 and outcome in long-term follow-up patients.

In conclusion, our study demonstrated that CCL2 promotes cardiomyocyte proliferation by activating CCR2/JNK/STAT3 signaling. Targeting CCL2 is a potential strategy for heart regeneration and cardiac repair after MI.

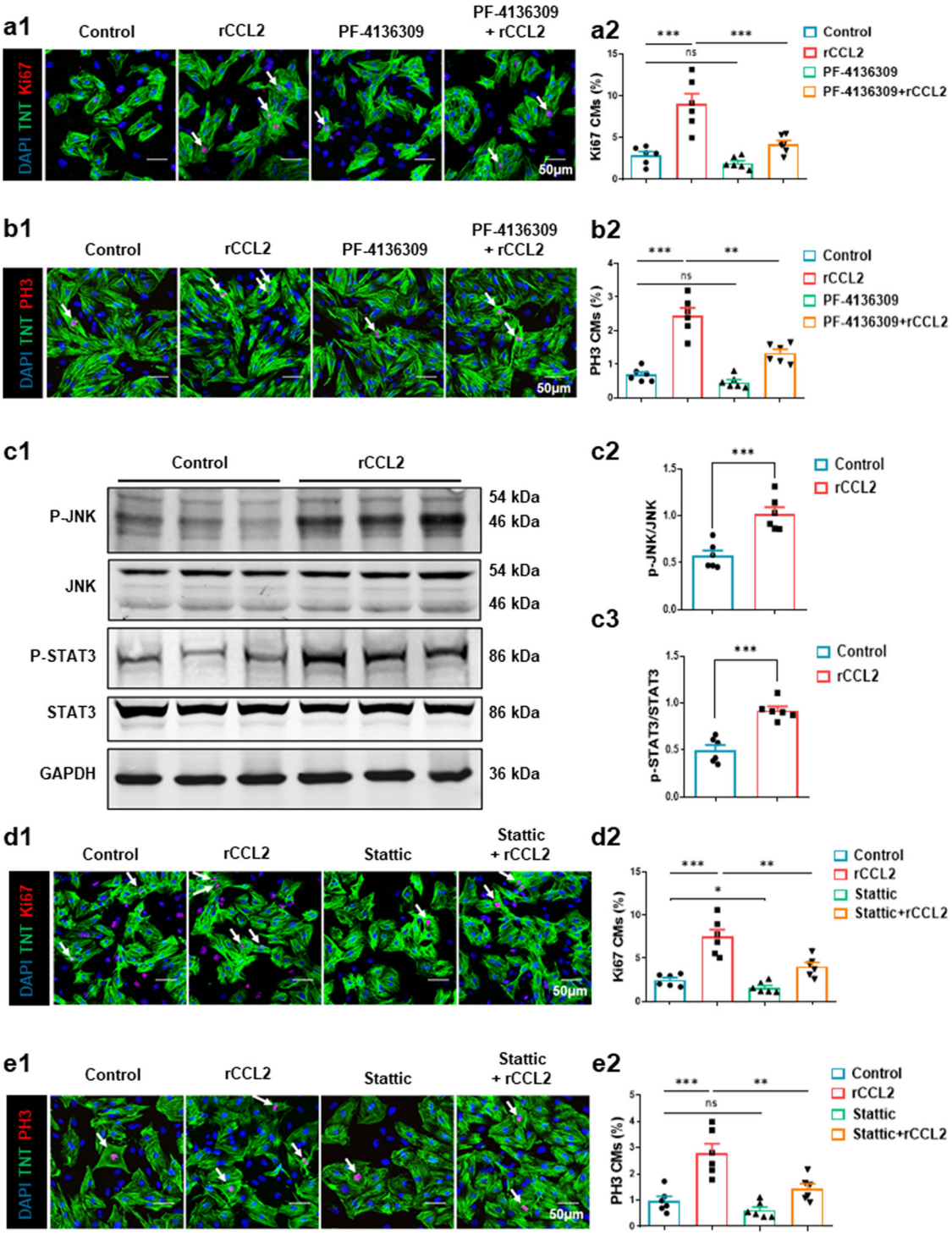

Fig. 6 Activation of STAT3 signaling in cardiomyocytes after recombinant CCL2 stimulation. a, b Representative immunofluorescence staining (**a1, b1**) and quantification (**a2, b2**) of Ki67 and PH3 in cardiomyocytes 24 h after recombinant CCL2 treatment (100 ng/mL) with or without PF-4136309 (30 μM), a CCR2 antagonist ($n = 6$, ns not significant, $^{**}P < 0.01$, $^{***}P < 0.001$, scale bar = 50 μm). **c** Representative immunoblot image (**c1**) and quantification (**c2**, **c3**) of p-JNK and p-STAT3 in cardiomyocytes after recombinant CCL2 administration ($n = 6$, ns. not significant, $^{***}P < 0.001$, scale bar = 50 μm). **d, e** Representative immunofluorescence staining **(d1, e1)** and quantification (**d2, e2**) of Ki67 and PH3 in cardiomyocytes 24 h after recombinant CCL2 treatment with or without Stattic (30 μM), a STAT3 phosphorylation inhibitor ($n = 6$, ns. not significant, $^{**}P < 0.01$, $^{***}P < 0.001$, scale bar = 50 μm). CMs cardiomyocytes.

ACKNOWLEDGEMENTS

This study was supported by grants from the National Natural Science Foundation of China (81930008, 81900792), the Natural Science Foundation of Chongqing (2023NSCQ-MSX2101), the National Key R&D Program of China (2018YFC1312700), the Program of Innovative Research Team by the National Natural Science Foundation (81721001), and the Program for Changjiang Scholars and Innovative Research Team in University; IRT1216.

AUTHOR CONTRIBUTIONS

WW, LPL, and CYZ conceived the study, designed the experiments and wrote the manuscript; WW performed immunofluorescence staining, enzyme-linked immunosorbent assays, real-time PCR, and endothelial tube formation assays; XKC generated the animal model and performed Masson staining analysis; LZ and FW performed echocardiography and evaluated heart function; YJH performed western blotting; BJL and ZXL performed data analysis; ZGH performed several experiments related to the animal model; XWX isolated and cultured primary cardiomyocytes; WEW, LPL and CYZ revised the manuscript. All authors approved the manuscript.

ADDITIONAL INFORMATION

Supplementary information The online version contains supplementary material available at https://doi.org/10.1038/s41401-023-01198-0.

Competing interests: The authors declare no competing interests.

REFERENCES

1. Reed GW, Rossi JE, Cannon CP. Acute myocardial infarction. Lancet. 2017;389:197–210.
2. Chablais F, Veit J, Rainer G, Jazwinska A. The zebrafish heart regenerates after cryoinjury-induced myocardial infarction. BMC Dev Biol. 2011;11:21.
3. Wang Z, Cui M, Shah AM, Ye W, Tan W, Min YL, et al. Mechanistic basis of neonatal heart regeneration revealed by transcriptome and histone modification profiling. Proc Natl Acad Sci USA. 2019;116:18455–65.
4. Uygur A, Lee RT. Mechanisms of cardiac regeneration. Dev Cell. 2016;36:362–74.
5. Bergmann O, Bhardwaj RD, Bernard S, Zdunek S, Barnabe-Heider F, Walsh S, et al. Evidence for cardiomyocyte renewal in humans. Science. 2009;324:98–102.
6. Yuan X, Braun T. Multimodal regulation of cardiac myocyte proliferation. Circ Res. 2017;121:293–309.
7. Aurora AB, Porrello ER, Tan W, Mahmoud AI, Hill JA, Bassel-Duby R, et al. Macrophages are required for neonatal heart regeneration. J Clin Invest. 2014;124:1382–92.
8. Singh S, Anshita D, Ravichandiran V. MCP-1: function, regulation, and involvement in disease. Int Immunopharmacol. 2021;101:107598.
9. Chen B, Frangogiannis NG. Chemokines in myocardial infarction. J Cardiovasc Transl Res. 2021;14:35–52.
10. de Lemos JA, Morrow DA, Sabatine MS, Murphy SA, Gibson CM, Antman EM, et al. Association between plasma levels of monocyte chemoattractant protein-1 and long-term clinical outcomes in patients with acute coronary syndromes. Circulation. 2003;107:690–5.
11. Zhu Y, Hu C, Du Y, Zhang J, Liu J, Han H, et al. Significant association between admission serum monocyte chemoattractant protein-1 and early changes in myocardial function in patients with first ST-segment elevation myocardial infarction after primary percutaneous coronary intervention. BMC Cardiovasc Disord. 2019;19:107.
12. Morimoto H, Takahashi M, Izawa A, Ise H, Hongo M, Kolattukudy PE, et al. Cardiac overexpression of monocyte chemoattractant protein-1 in transgenic mice prevents cardiac dysfunction and remodeling after myocardial infarction. Circ Res. 2006;99:891–9.
13. Quaife-Ryan GA, Sim CB, Ziemann M, Kaspi A, Rafehi H, Ramialison M, et al. Multicellular transcriptional analysis of mammalian heart regeneration. Circulation. 2017;136:1123–39.
14. Whitehead AJ, Engler AJ. Regenerative cross talk between cardiac cells and macrophages. Am J Physiol Heart Circ Physiol. 2021;320:H2211–H21.
15. Qian Y, Ding P, Xu J, Nie X, Lu B. CCL2 activates AKT signaling to promote glycolysis and chemoresistance in glioma cells. Cell Biol Int. 2022;46:819–28.
16. Keeley EC, Mehrad B, Strieter RM. Chemokines as mediators of neovascularization. Arterioscler Thromb Vasc Biol. 2008;28:1928–36.
17. Li X, Sun X, Carmeliet P. Hallmarks of endothelial cell metabolism in health and disease. Cell Metab. 2019;30:414–33.
18. Ge S, Shrestha B, Paul D, Keating C, Cone R, Guglielmotti A, et al. The CCL2 synthesis inhibitor bindarit targets cells of the neurovascular unit, and suppresses experimental autoimmune encephalomyelitis. J Neuroinflammation. 2012;9:171.
19. Tian DS, Peng J, Murugan M, Feng LJ, Liu JL, Eyo UB, et al. Chemokine CCL2-CCR2 signaling induces neuronal cell death via STAT3 activation and IL-1beta production after status epilepticus. J Neurosci. 2017;37:7878–92.
20. Yao M, Fang W, Smart C, Hu Q, Huang S, Alvarez N, et al. CCR2 chemokine receptors enhance growth and cell-cycle progression of breast cancer cells through SRC and PKC activation. Mol Cancer Res. 2019;17:604–17.
21. Fang Y, Gupta V, Karra R, Holdway JE, Kikuchi K, Poss KD. Translational profiling of cardiomyocytes identifies an early Jak1/Stat3 injury response required for zebrafish heart regeneration. Proc Natl Acad Sci USA. 2013;110:13416–21.
22. Uchihara Y, Ohe T, Mashino T, Kidokoro T, Tago K, Tamura H, et al. N-Acetyl cysteine prevents activities of STAT3 inhibitors, Stattic and BP-1-102 independently of its antioxidant properties. Pharmacol Rep. 2019;71:1067–78.
23. Eschenhagen T, Bolli R, Braun T, Field LJ, Fleischmann BK, Frisen J, et al. Cardiomyocyte regeneration: a consensus statement. Circulation. 2017;136:680–6.
24. Senyo SE, Steinhauser ML, Pizzimenti CL, Yang VK, Cai L, Wang M, et al. Mammalian heart renewal by pre-existing cardiomyocytes. Nature. 2013;493:433–6.
25. Nian M, Lee P, Khaper N, Liu P. Inflammatory cytokines and postmyocardial infarction remodeling. Circ Res. 2004;94:1543–53.
26. Frangogiannis NG, Dewald O, Xia Y, Ren G, Haudek S, Leucker T, et al. Critical role of monocyte chemoattractant protein-1/CC chemokine ligand 2 in the pathogenesis of ischemic cardiomyopathy. Circulation. 2007;115:584–92.
27. Georgakis MK, Bernhagen J, Heitman LH, Weber C, Dichgans M. Targeting the CCL2-CCR2 axis for atheroprotection. Eur Heart J. 2022;43:1799–808.
28. Dewald O, Zymek P, Winkelmann K, Koerting A, Ren G, Abou-Khamis T, et al. CCL2/monocyte chemoattractant protein-1 regulates inflammatory responses critical to healing myocardial infarcts. Circ Res. 2005;96:881–9.
29. Zhang W, Zhu T, Chen L, Luo W, Chao J. MCP-1 mediates ischemia-reperfusion-induced cardiomyocyte apoptosis via MCPIP1 and CaSR. Am J Physiol Heart Circ Physiol. 2020;318:H59–H71.
30. Zhou L, Azfer A, Niu J, Graham S, Choudhury M, Adamski FM, et al. Monocyte chemoattractant protein-1 induces a novel transcription factor that causes cardiac myocyte apoptosis and ventricular dysfunction. Circ Res. 2006;98:1177–85.
31. Li Y, Feng J, Song S, Li H, Yang H, Zhou B, et al. gp130 controls cardiomyocyte proliferation and heart regeneration. Circulation. 2020;142:967–82.
32. Miyawaki A, Obana M, Mitsuhara Y, Orimoto A, Nakayasu Y, Yamashita T, et al. Adult murine cardiomyocytes exhibit regenerative activity with cell cycle reentry through STAT3 in the healing process of myocarditis. Sci Rep. 2017;7:1407.
33. Osugi T, Oshima Y, Fujio Y, Funamoto M, Yamashita A, Negoro S, et al. Cardiac-specific activation of signal transducer and activator of transcription 3 promotes vascular formation in the heart. J Biol Chem. 2002;277:6676–81.
34. Hilfiker-Kleiner D, Hilfiker A, Drexler H. Many good reasons to have STAT3 in the heart. Pharmacol Ther. 2005;107:131–7.
35. Hilfiker-Kleiner D, Hilfiker A, Fuchs M, Kaminski K, Schaefer A, Schieffer B, et al. Signal transducer and activator of transcription 3 is required for myocardial capillary growth, control of interstitial matrix deposition, and heart protection from ischemic injury. Circ Res. 2004;95:187–95.
36. Combadiere C, Potteaux S, Rodero M, Simon T, Pezard A, Esposito B, et al. Combined inhibition of CCL2, CX3CR1, and CCR5 abrogates Ly6C(hi) and Ly6C(lo) monocytosis and almost abolishes atherosclerosis in hypercholesterolemic mice. Circulation. 2008;117:1649–57.
37. Owsiany KM, Deaton RA, Soohoo KG, Tram Nguyen A, Owens GK. Dichotomous roles of smooth muscle cell-derived MCP1 (monocyte chemoattractant protein 1) in development of atherosclerosis. Arterioscler Thromb Vasc Biol. 2022;42:942–56.